Available online at www.sciencedirect.com

SCIENCE DIRECT

Biochimica et Biophysica Acta 1667 (2004) 38–46

BIOCHIMICA ET BIOPHYSICA ACTA BBA

http://www.elsevier.com/locate/bba

Oligomerization triggers binding of a *Bacillus thuringiensis* Cry1Ab pore-forming toxin to aminopeptidase N receptor leading to insertion into membrane microdomains

A. Bravo[a,*], I. Gómez[a], J. Conde[a], C. Muñoz-Garay[a], J. Sánchez[a], R. Miranda[a], M. Zhuang[b], S.S. Gill[b], M. Soberón[a]

[a]*Instituto de Biotecnología, Universidad Nacional Autónoma de México, Apdo. Postal 510-3, Cuernavaca 62250, Morelos, México*
[b]*Department of Cell Biology and Neuroscience, University of California, Riverside, CA 92521, USA*

Received 6 May 2004; received in revised form 16 August 2004; accepted 30 August 2004
Available online 11 September 2004

Abstract

Bacillus thuringiensis Cry1A toxins, in contrast to other pore-forming toxins, bind two putative receptor molecules, aminopeptidase N (APN) and cadherin-like proteins. Here we show that Cry1Ab toxin binding to these two receptors depends on the toxins' oligomeric structure. Toxin monomeric structure binds to Bt-R_1, a cadherin-like protein, that induces proteolytic processing and oligomerization of the toxin (Gómez, I., Sánchez, J., Miranda, R., Bravo A., Soberón, M., FEBS Lett. (2002) 513, 242–246), while the oligomeric structure binds APN, which drives the toxin into the detergent-resistant membrane (DRM) microdomains causing pore formation. Cleavage of APN by phospholipase C prevented the location of Cry1Ab oligomer and Bt-R_1 in the DRM microdomains and also attenuates toxin insertion into membranes despite the presence of Bt-R_1. Immunoprecipitation experiments demonstrated that initial Cry1Ab toxin binding to Bt-R_1 is followed by binding to APN. Also, immunoprecipitation of Cry1Ab toxin-binding proteins using pure oligomeric or monomeric structures showed that APN was more efficiently detected in samples immunoprecipitated with the oligomeric structure, while Bt-R_1 was preferentially detected in samples immunoprecipitated with the monomeric Cry1Ab. These data agrees with the 200-fold higher apparent affinity of the oligomer than that of the monomer to an APN enriched protein extract. Our data suggest that the two receptors interact sequentially with different structural species of the toxin leading to its efficient membrane insertion.

Keywords: *Bacillus thuringiensis*; Mode of action; Aminopeptidase; Cadherin; Lipid raft; Oligomer

1. Introduction

Bacillus thuringiensis (Bt) produces insecticidal proteins (Cry protoxins) during sporulation as parasporal crystals. Bt toxins are widely used as bioinsecticides since they are specific to their target insects, are safe to other animals and plants, and are biodegradable [1]. As a result, insect-resistant transgenic plants, which express Cry proteins, are now extensively used for cotton and corn production [1]. However, despite the widespread use of Bt and transgenic crops, the precise mechanism of action of Cry proteins is incompletely understood. In particular, the role of two different receptors, aminopeptidase N (APN) and cadherin-like proteins (BT-R_1 in *Manduca sexta*) remains to be determined.

The primary action of Cry toxins is to lyse midgut epithelial cells in the target insect by forming lytic pores in the apical membrane [1]. The three-dimensional structures of some Cry toxins have been resolved [2–4] showing that

Abbreviations: Bt, *Bacillus thuringiensis*; Cry, crystal proteins; APN, aminopeptidase N; Bt-R_1, *Manduca sexta* cadherin-like receptor; Bt-R_{175}, *Bombyx mori* cadherin-like receptor; DRM, detergent-resistant membranes; BBMV, brush border membrane vesicles; GPI, glycosylphosphatidylinositol; PI-PLC, phosphatidylinositol phospholipase C; PMSF, phenylmethanesulfonyl fluoride; PVDF, polyvinylidene difluoride; HRP, horseradish peroxidase; ELISA, enzyme-linked immunosorbent assay; K_D, equilibrium dissociation constant

* Corresponding author. Tel.: +52 7329 1635; fax: +52 777 317 2388.
E-mail address: bravo@ibt.unam.mx (A. Bravo).

0005-2736/$ - see front matter © 2004 Elsevier B.V. All rights reserved.
doi:10.1016/j.bbamem.2004.08.013

they are comprised of three domains. Domain I, a seven-α helix bundle, is the pore-forming domain, while domains II and III, composed of β-sheets, are apparently involved in receptor binding [1–4]. The Cry1Aa, Cry1Ab and Cry1Ac proteins, which share more than 85% amino acid sequence identity as protoxins, are selectively toxic to some lepidopteran insect pests. These Cry1A toxins bind to the same receptor molecules (APN and BT-R) suggesting they have a similar mode of action [5–10]. Domain I in these toxins is similar, but domains II and III show important sequence differences. Because different lepidopteran insects show varying sensitivity to these Cry1A toxins, it is likely that the differences in domain II and III influence the receptor binding affinity and activity of these toxins.

Cry protoxins must go through several structural changes before reaching their functional pore-forming state: (1) solubilization of crystal proteins and activation of the protoxin by midgut proteases, resulting in the production of monomeric toxin. In the case of the Cry1A toxins, the 130 kDa protoxin is cleaved to a ~60 kDa toxin. (2) Binding of the toxin to specific membrane receptors on the apical membrane of midgut cells [11,12]. In lepidopteran insects, the Cry1A toxins bind to a 120 kDa APN [5–8], and to a cadherin-like protein of 210 kDa (Bt-R_1) in *M. sexta* [9] or in the case of *Bombyx mori* to a 175 kDa protein (Bt-R_{175}) [10]. Differences in binding affinities between APN (100 nM) [7] and Bt-R_1 (1 nM) [13] to Cry1Ab toxin suggest that binding to Bt-R_1 is likely the first event in Cry1Ab toxin interaction with microvilli membranes. (3) Formation of a pre-pore oligomeric structure, probably a tetramer, by intermonomeric contacts and subsequent insertion into the apical membrane to make active lytic pores [14–18].

Binding to BT-R cadherin-like receptors is an important step in the mode of action of Cry1A toxins. Expression of the Bt-R_{175} receptor in lepidopteran cells renders them sensitive to the Cry1A toxin [10]. However, expression of Bt-R_1 or Bt-R_{175} in other cell types requires very high Cry1A toxin levels to cause cell lysis in a small proportion of cells expressing the receptor [19–21], suggesting that additional factors in the larval midgut could contribute to toxicity [21]. Cry1Aa toxin lyses midgut epithelial cells from *B. mori* larvae, and this toxic effect was inhibited if the cells were preincubated with anti-Bt-R_{175} antisera [22]. More importantly, disruption of the cadherin-like gene by a retrotransposon-mediated insertion contributed 40–80% of the Cry1Ac resistance levels in *H. virescens* YHD2 larvae [23]. In addition, Cry1Ab toxin binding to Bt-R_1 induces the cleavage of helix α-1 and the formation of a pre-pore oligomeric structure that is accompanied by exposure of hydrophobic surfaces [14]. This cleavage would result in 3 kDa reduction in size of the toxin [24]. We previously showed that this Cry1Ab oligomer is active in bioassays against *M. sexta* [14], and that it inserts more efficiently into membrane vesicles, in contrast to the monomeric Cry1Ab, forming stable channels with high open probability [15], suggesting that the oligomer is required for proper toxin insertion into membranes [15].

The data above, therefore, suggests that APNs are not critical for toxicity. However, recent evidence also supports an important role for APNs in Cry1 toxicity. For example, reduced expression of an APN, by gene silencing using dsRNA in vivo, decreased the Cry1C toxicity to *Spodoptera litura* [25]. In addition, heterologous expression of *M. sexta* APN in the midgut and mesodermal tissues of transgenic *Drosophila melanogaster* resulted in increased sensitivity to Cry1Ac toxin [26]. Finally, APN incorporation into lipid bilayers enhanced Cry1Aa pore-formation activity [27].

All Cry1A-APN receptors are anchored to the membrane by a glycosylphosphatidylinositol (GPI) anchor [5–8]. Phosphatidylinositol phospholipase C (PI-PLC) treatment of *Trichoplusia ni* brush border membrane vesicles (BBMV), resulting in cleavage of GPI-anchored proteins from membrane, drastically reducing the pore-formation activity of Cry toxins [28]. These GPI-anchored proteins are selectively included in lipid rafts that are conceived as spatially differentiated liquid-ordered microdomains in cell membranes [29]. Lipid rafts are detergent-resistant membranes (DRM) enriched in glycosphingolipids, cholesterol and GPI-anchored proteins and are involved in signal transduction, sorting and trafficking of plasma membrane proteins in mammalian cells [29]. Also, they function as pathogen portals for different viruses, bacteria and toxins [30,31]. Recently, we demonstrated that the APNs in *M. sexta* and *H. virescens*, in contrast to the cadherin receptors, are located in DRM, and that the integrity of these microdomains is essential for Cry1Ab pore activity [32].

In this work we provide evidence that the cadherin-like proteins and APNs are sequentially involved in Cry1A toxicity. We also show that the oligomeric pre-pore structure has increased affinity for APN, compared to that of the monomer. This increased affinity for APN facilitates the mobilization of the Cry1A pre-pore to the site of toxin insertion in the apical membrane, the DRM microdomains.

2. Materials and methods

2.1. Cry1Ab toxin purification

Cry1Ab crystals were produced in the acrystalliferous *Bt* strain 407 *cry*$^-$ transformed with pHT315 plasmid [33] harbouring the *cry*1Ab gene (pHT315-1Ab). This Bt strain was grown for 3 days at 29 °C in nutrient broth sporulation medium supplemented with 10 μg/ml erythromycin. After sporulation, crystals were purified by sucrose gradients as reported [14] and the crystals were solubilized in 50 mM Na_2CO_3 pH 10.5, 0.2% β-mercaptoethanol. The resulting protoxin was activated as described [14]. Briefly, the protoxin was incubated for 1 h with scFv73 antibody in a mass ratio 1:4 and digested with midgut juice (5%) for 1 h at 37 °C. Phenylmethanesulfonyl fluoride (PMSF, 1 mM) was added to stop the reaction. The monomeric and oligomeric forms of Cry1Ab were purified by size-exclusion chroma-

tography in Superdex 200 HR 10/30 (Amersham Pharmacia Biotech, Uppsala, Sweden) FPLC size-exclusion as previously reported [14,15].

2.2. Preparation of BBMV

M. sexta eggs were reared on artificial diet. BBMV from fifth instar larvae were prepared as reported without protease inhibitors [16] and the BBMV preparation was finally suspended in TNE buffer (25 mM Tris–HCl, 150 mM NaCl, 5 mM EDTA pH 7.4).

2.3. Purification of DRM microdomains

BBMV (1 mg protein) were incubated for 1 h at 25 °C with or without soluble Cry1Ab protoxin (100 μg) in TNE. Alternatively, BBMV were incubated with 10 U PI-PLC during 1 h at 30 °C, centrifuged 10 min at 14,000 rpm, 4 °C (Eppendorf 5804R) to remove the released GPI-anchored proteins and PI-PLC, and then incubated for 1 h with Cry1Ab protoxin (100 μg) as described above. After incubation with protoxin, 1 mM PMSF was added, and the unbound Cry1Ab was washed out with TNE buffer by centrifugation of the membranes 10 min at 14,000 rpm 4 °C. The pellet membrane was suspended in 360 μl of cold TNE buffer containing 1% Triton X-100 and protease inhibitors (0.2 mM PMSF, 100 μg/ml of leupeptin and pepstatin), and incubated 30 min at 4 °C. The samples were adjusted to 40% iodixanol with 715 μl Optiprep (Sigma-Aldrich), and overlaid with 3 ml of 30% iodixanol in TNE, followed by 0.2 ml of TNE. The gradients were centrifuged at 268,000×*g* for 2 h at 4 °C. Fractions of 0.5 ml were collected. Under these conditions, the Triton X-100-soluble fraction was found at the bottom of the tube, while the insoluble DRM buoyant fraction was at the interphase between 30% and 0% iodixanol.

2.4. Detection of APN, Cry1Ab and Bt-R_1 by Western blot

The proteins from insoluble and soluble membrane fractions of the iodixanol Optiprep flotation gradients were separated by 9% SDS-PAGE and blotted onto polyvinylidene difluoride (PVDF) Immobilon membranes (Amersham Biosciences). The blots were blocked with 5% powdered milk in phosphate-buffered saline (PBS; 50 mM potassium phosphate buffer, pH 7.4, 0.1 M NaCl) and 0.05% Tween 20 and incubated with anti-APN antibody (1:10,000), kindly supplied by Dr. Michael Adang (Athens, GA), or anti-*H. virescens* BT-R_1 antibody (1:1,000), or anti-Cry1Ab antibody (1:40,000) followed by incubation with anti-rabbit horseradish peroxidase (HRP; 1:5000) secondary antibody (goat anti-rabbit, Sigma). Blots were developed by enhanced chemiluminescence (ECL, Amersham Biosciences). Molecular weight markers used in all SDS-PAGE were precision plus standards, all blue (BioRad) or full range rainbow (Amersham Biosciences). The advantage of using these pre-stained proteins is that they are easily observed even when blotted into PVDF membranes. Western blot analysis of soluble and DRM membrane proteins were done at least three times. Representative results are presented.

2.5. Immunoprecipitation of Cry1Ab or aminopeptidase

Three microliters of anti-Cry1Ab or 1.5 μl of anti-APN polyclonal antibodies were incubated 1 h at 4 °C with 100 μl of protein A-Sepharose CL-4B beads (Pharmacia) in PBS. Then the protein-A-Sepharose beads were washed three times with PBS by 10 min centrifugation at 14,000 rpm 4 °C. BBMV (1 mg protein) were incubated with soluble Cry1Ab protoxin (100 μg) for 0, 5 and 15 min, and after incubation, 1 mM PMSF was added and membranes were centrifuged 10 min at 14,000 rpm to remove unbound toxin. The membrane pellets were solubilized 1 h at 25 °C in 100 μl of PBS, 1 mM PMSF, 40 mM CHAPS and 10 mM $CaCl_2$. The samples were again centrifuged 10 min at 14,000 rpm and the supernatants containing the solubilized BBMV proteins were added to 100 μl of protein A-Sepharose beads previously linked to anti-Cry1Ab or to anti-APN antibodies. The samples were incubated 12 h at 4 °C. Protein A-Sepharose beads were pelleted and washed six times with PBS. The bound-complex was dissociated from the beads by boiling in SDS-solubilization Laemmli buffer and separated by 9% SDS-PAGE, including molecular weight markers as above and the associated proteins were visualized by Western blot. The bands observed in the Western blot were analyzed by scanning optical density. Immunoprecipitation experiments were performed three times.

2.6. Immunoprecipitation of Cry1Ab binding proteins

To immunoprecipitate the Cry1Ab binding proteins, Bt-R_1 and APN, 3 μl of anti-Cry1Ab polyclonal antibody were incubated with protein A-Sepharose CL-4B in PBS as above. After washing steps, pure monomeric or oligomeric Cry1Ab structures (200 nM) that were purified by size exclusion chromatography as described above were added. The two mixtures were incubated 1 h at 4 °C and washed again three times with PBS. BBMV proteins (1 mg protein) were solubilized with CHAPS as described above and the solubilized proteins were incubated 12 h at 4 °C with 100 μl of the complex formed by protein A-Sepharose beads linked to pure monomeric or oligomeric Cry1Ab. Finally, Sepharose beads were pelleted and washed six times with PBS. The binding-complex was dissociated from the beads by boiling for 3 min in SDS-solubilization Laemmli buffer, separated by 9% SDS-PAGE, including molecular weight markers as above and the associated proteins were visualized by Western blot using specific antibodies. The APN and Bt-R1 bands obtained in the Western blot were analyzed by scanning optical density. The error observed in the different experiments duplications was less than 10%.

2.7. Determination of Cry1Ab oligomer and monomer affinities to APN-enriched protein extract by competition ELISA

To measure the kinetics of association of monomeric and oligomeric structures of Cry1Ab to APN, BBMV were solubilized as described for *Lymantria dispar* APN purification [34]. This procedure resulted in 50-fold increase in APN-specific activity. Apparent dissociation constants (K_D) were determined by competitive enzyme-linked immunosorbent assay (ELISA) as described [35,36]. Ten nanomoles of Cry1Ab monomeric or oligomeric structures (equivalent to the monomeric concentration) were equilibrated with increasing concentrations of APN-enriched extract (from 0.25 nM to 1 μM estimated APN concentration, based on APN molecular weight and protein concentration) in 100 μl PBS for 1 h at 25 °C. For BBMV binding analysis similar units of APN as the ones used for the APN-enriched extract were equilibrated with the monomer. The incubation mixtures were transferred to a 96-well ELISA plate previously coated with 2.5 μg APN-enriched extract to determine the amount of unbound Cry1Ab structures. The ELISA plates were washed three times and detected with anti-Cry1Ab antibody (1:1000) followed by a secondary goat-anti-rabbit-HRP antibody and detected by HRP enzymatic activity. The concentration of APN at which the half-maximal ELISA signal is detected corresponds to the dissociation constant [35,36]. Concentrated preparations of pure Cry1Ab oligomeric structure could form aggregates in a concentration-dependent manner [15]. For this reason, we used a 10 nM concentration of oligomeric structure that remains stable [15].

3. Results

3.1. Localization of APN, BT-R_1 and Cry1Ab toxin in DRM

Recently we demonstrated that APN and Cry1A toxins co-localized in DRM microdomains of *M. sexta* and *H. virescens* [32]. The co-localization of Cry1A and APN in DRM suggested that APN could drive the Cry1A toxins to these membrane microdomains. To answer this question, *M. sexta* BBMV were isolated and treated 1 h with PI-PLC that cleaves out GPI-anchored proteins in the vesicles. After washing the excess PI-PLC by centrifugation, BBMV were incubated 1 h with soluble Cry1Ab protoxin (130 kDa) in the absence of protease inhibitors. Then BBMV were centrifuged and DRM purified as described in Purification of DRM microdomains. The presence of Cry1Ab toxin, Bt-R_1 and APN in DRM membranes was determined by Western blots. Control treatments without PI-PLC incubation included BBMV incubated with or without Cry1Ab protoxin. Fig. 1A shows that in BBMV incubated without Cry1Ab protoxin, the Bt-R_1 receptor was associated with the soluble membrane fraction in contrast to APN which

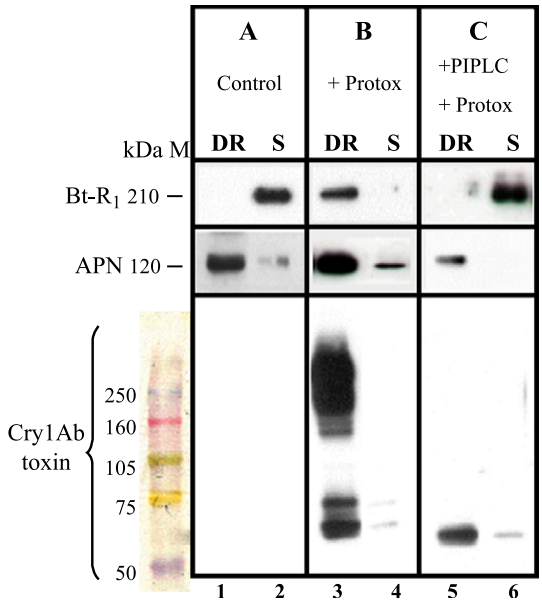

Fig. 1. Interaction of Cry1Ab toxin with its receptors. BBMV were incubated 1 h with/without Cry1Ab protoxin (100 μg/mg BBMV), unbound toxin was washed and DRM purified. Panel A, control BBMV without protoxin incubation. Panel B, BBMV treated with Cry1Ab protoxin. Panel C, BBMV were preincubated 1 h with PIPLC (10 U/mg BBMV) washed by centrifugation, then treated 1 h with protoxin, washed again and DRM purified. Immunodetection was done with anti-BT-R_1 (α-BT-R_1), anti-APN (α-APN) or anti-Cry1Ab (α-Cry1Ab) antibodies. DR, detergent-resistant membranes purified by Optiprep flotation gradients; S, soluble membranes. M, pre-stained molecular weight markers.

was enriched in the detergent-resistant fraction, as previously reported [32]. In contrast, in BBMV incubated with protoxin, the distribution of the Bt-R_1 receptor changed, since most Bt-R_1 is now associated with the insoluble DRM membranes (Fig. 1B). We also observed the Cry1Ab protoxin was processed by membrane-associated proteases because most of the Cry1Ab detected in insoluble DRM had either a 60 or 250 kDa molecular size, which corresponds to the activated monomeric and oligomeric forms of the toxin, respectively [14]. Finally, pretreatment of BBMV with PI-PLC substantially reduced the amount of APN present in the DRM. Bt-R_1 and Cry1Ab were also reduced in the insoluble DRM fractions after PI-PLC treatment (Fig. 1C). Surprisingly, the total amount of Cry toxin bound to DRM or to soluble membranes was severely reduced after APN cleavage by PI-PLC, indicating that APN might also be involved in toxin insertion into the membrane.

3.2. Interaction of APN and Bt-R_1 with oligomeric and monomeric structures of Cry1Ab toxin

The presence of APN and Bt-R_1 receptors and the Cry1Ab 250 kDa oligomer in DRM microdomains suggests that these three proteins are, at some time, forming a complex. To analyze the time course of this interaction of Cry1Ab toxin with the two receptors, *M. sexta* BBMV were incubated with soluble Cry1Ab protoxin for 0, 5 and 15

min. Time 0 corresponds to the mixing of protoxin and BBMV that were immediately processed by centrifugation for the immunoprecipitation of Cry1Ab toxin as described in Materials and methods. After removal of unbound toxin by centrifugation, the membrane pellet was solubilized with CHAPS and used to immunoprecipitate Cry1Ab toxin with an anti-Cry1Ab polyclonal antibody linked to protein A-Sepharose beads, and the co-precipitation of APN and Bt-R_1 was analyzed by Western blot. Fig. 2A shows that the anti-Cry1Ab antibody precipitated the Cry1Ab activated toxin at all times tested, including time 0, suggesting that the activation of the protoxin is very efficient, However, it is important to note that time 0 implies a 10-min centrifugation step and this time is long enough to activate the protoxin. Two different bands of ~60 and 65 kDa were detected, which corresponds to Cry1Ab toxin [24,37]. At time 15 min, we observed the presence of detectable amounts of oligomeric structure. Fig. 2B depicts the co-precipitation of Bt-R_1, detected with anti-Bt-R_1 antibody, showing that Bt-R_1 was co-precipitated with Cry1Ab toxin and the amount of Bt-R_1 was comparable at all times tested. In contrast, APN was preferentially co-precipitated only at 5 and 15 min (Fig. 2C). Quantification of blot bands indicated that there was a 4-fold progressive increase in the amount of APN (Fig. 2C) and a slight decrease in the amount of Bt-R_1 that co-precipitated with the toxin (Fig. 2B). The deviation in the obtained values of both receptors between different experiment repetitions was 5%. Fig. 2A shows lower amounts of IgG than Fig. 2B and C since the blot of Fig. 2A was exposed to the film for a short time period (less than 1 min), after treatment with enhanced chemiluminescence in order to distinguish monomeric toxin from IgG molecule. Fig. 2 also shows that the polyclonal anti-Cry1Ab used does not cross-react either with BT-R_1 or with APN, since in control lanes performed without Cry1Ab protoxin incubation (labelled C), no signal of both receptors were detected after immunoprecipitation. These data suggest that interaction of the toxin with receptors is very fast with the first contact occurring with Bt-R_1, as observed at 0 time.

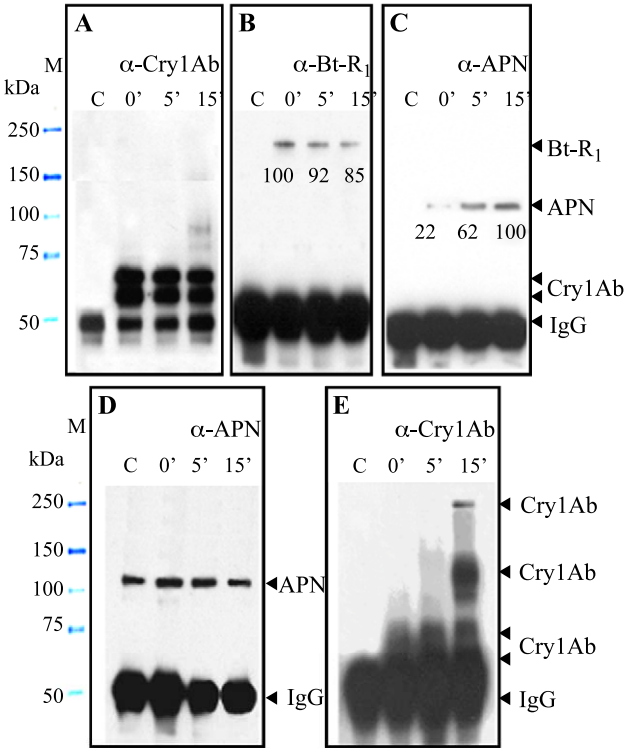

Fig. 2. Immunoprecipitation of Cry1Ab and APN from BBMV incubated with Cry1Ab protoxin. Immunoprecipitation of Cry1Ab or APN from BBMV incubated 0, 5 or 15 min with Cry1Ab protoxin by adding protein A-Sepharose-anti-Cry1Ab (panels A, B and C) or protein A-Sepharose-anti-APN (panels D and E). The precipitates were dissociated in SDS-PAGE and co-precipitated proteins detected by Western blot. Panel A, samples of the Cry1Ab immunoprecipitated proteins analyzed with anti-Cry1Ab antibody (α-Cry1Ab). Panel B, same samples analyzed with anti-BT-R_1 antibody (α-BT-R_1). Panel C, same samples analyzed with anti-APN antibody (α-APN). Panel D, samples of the APN immunoprecipitated proteins analyzed with anti-APN antibody. Panel E, same samples analyzed with anti-Cry1Ab antibody. Lane C, controls of BBMV without protoxin incubation. M, pre-stained molecular weight markers. Numbers within the images represent the percentage of Bt-R_1 signal at time 0 or APN signal at time 15 min as determined by scanning optical density of bands in the blots.

In order to gain additional evidence of possible interaction of Cry1Ab with APN receptor, APN was immunoprecipitated from the same samples and toxin was detected. Fig. 2D shows that APN was immunoprecipitated at all times tested. However, the oligomeric Cry1Ab toxin co-precipitated with APN only in longer incubation times in contrast to the monomeric toxin that co-precipitated with APN at short incubation times (Fig. 2E).

3.3. Differential interaction of monomeric and oligomeric structures of Cry1Ab with the two receptors

In order to analyze the interaction of monomeric and oligomeric Cry1Ab with both receptors, pure monomeric or oligomeric structures (200 nM) were linked to protein A-Sepharose beads and used to immunoprecipitate Cry1Ab binding proteins from solubilized BBMV (1 mg). Previously we determined that 10 μg of BBMV saturated the binding of 10 nM Cry1Ab toxin. Therefore, we used 5-fold higher BBMV concentration to insure that all toxin molecules will interact with toxin receptors. The co-precipitation of APN and Bt-R_1 with pure oligomeric or monomeric structures of Cry1Ab was analyzed by Western blot using anti-APN- or anti-Bt-R_1-specific antibodies. Fig. 3A is a control showing the detection of Cry1Ab toxin after immunoprecipitation. In this figure, only monomeric and oligomeric toxins were detected correspondingly, indicating that only pure oligomeric or monomeric structures were coupled to the protein A-Sepharose beads. The results in Fig. 3B show that a greater amount of APN was detected after immunoprecipitation with the oligomeric structure. In contrast, the Bt-R_1 receptor was primarily immunoprecipitated with the monomeric form of the toxin (Fig. 3C). We tried to have similar amounts of IgG in all cases in order to support that the differences observed are likely due to

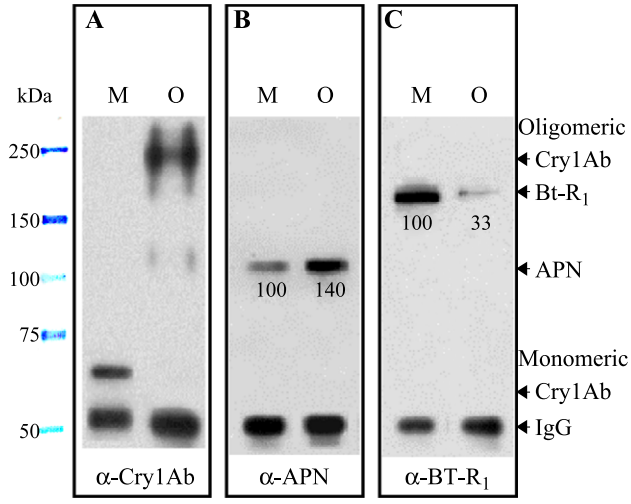

Fig. 3. Immunoprecipitation of the Cry1Ab binding proteins. The Cry1Ab binding proteins were precipitated by adding protein-A-sepharose-anti-Cry1Ab antisera-coupled to pure oligomeric Cry1Ab (lanes O) or coupled to pure monomeric Cry1Ab (lanes M). The precipitates were dissolved in SDS-solubilization buffer and the dissociated proteins were analyzed by SDS-PAGE. Panel A, the Cry1Ab monomeric or oligomeric toxins used in the immunoprecipitation experiments were detected by Western blot with anti-Cry1Ab antibody. The binding proteins present in the same samples were detected by Western blot using anti-APN (panel B) or anti-BT-R_1 (panel C) antibodies. Numbers within the images represent the percentage of Bt-R_1 or APN signal as determined by scanning optical density of bands in the blots.

differential interaction of the monomer and oligomer structures of the toxin structures with the two receptors.

3.4. Determination of dissociation constants of oligomeric and monomeric structures to enriched APN-membrane preparations

To further characterize the interaction of oligomeric and monomeric structures with APN, BBMV and protein extracts enriched in APN were used to determine the dissociation constant of Cry1Ab structures by competition ELISA [35,36]. Protein extracts enriched in APN were prepared as described [34]. After solubilization, APN-specific activities revealed a 50-fold increase than in BBMV and Cry1Ab ligand blot and Western blot analysis showed that the BT-R_1 protein was absent in this preparation (data not shown). Cry1Ab monomeric or oligomeric structures were equilibrated with increasing concentrations of APN-enriched extracts or with BBMV. The incubation mixtures were transferred to ELISA plates previously coated with an excess of APN extract to quantify the Cry1Ab toxin that remains in solution. Fig. 4 shows an apparent dissociation constant (K_D) of 165 nM for the monomer to the protein extract containing only APN. In contrast, the oligomer structure showed an apparent K_D of 0.75 nM to the APN-extract. Monomer binding to BBMV, showed in the insert of Fig. 3, revealed an apparent dissociation constant of 1.25 nM very similar to the reported K_D for BBMV [3].

4. Discussion

Pathogen interaction with target cells involves, in most cases, binding to specific receptors that trigger either membrane insertion or cell internalization through membrane microdomains. With viruses, human immunodeficiency virus [38], hepatitis C [39], and adenovirus [40] or bacteria like *Listeria* [41], this interaction involves multiple receptors, which could act together either to modulate each other or to contribute complementary functions. Alternatively, receptors might act sequentially. In the case of viruses, sequential binding to receptors is triggered by conformational changes in the binding proteins [39,40]. In contrast, single receptors seem to be a common feature for the interaction of bacterial pore-forming toxins with their target membranes. Nevertheless, for some toxins like anthrax, protective antigen [42], aerolysin [43,44] or diphtheria [45], more than one receptor molecule may participate. Anthrax protective antigen interacts with two receptors that share 60% identity [42], and it is believed that both receptors are interchangeable since cells expressing either one are sensitive to the toxin [42]. For aerolysin, the first binding event with cell surface carbohydrate moieties precedes binding to the GPI anchor [43,44]. For diphtheria toxin, CD9 enhances toxin binding to the diphtheria receptor [45].

Here we show for the first time the sequential involvement of two receptor molecules in the interaction of Cry1Ab toxin with its target cell membrane. Cry1Ab toxin first binds to Bt-R_1, thereby triggering toxin oligomerization resulting in a change in toxin affinity to the GPI-anchored APN. This

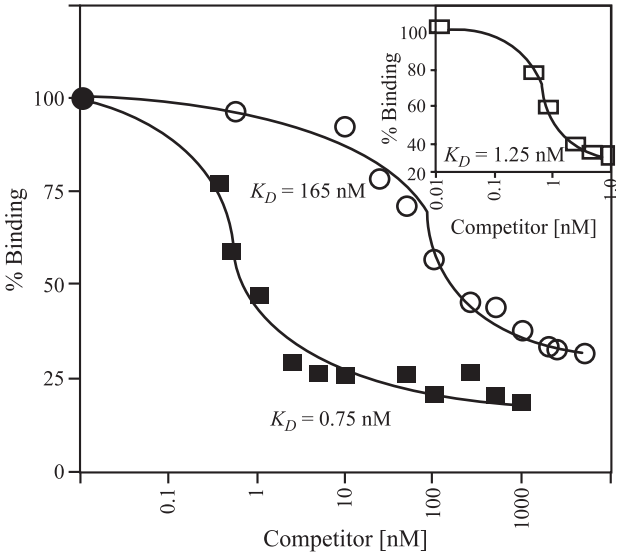

Fig. 4. Dissociation constants of APN-enriched protein extract to monomer (○) or to oligomer (■). Different molar concentrations (0.25 nM–1 μM) of APN-enriched extract were equilibrated with monomeric or oligomeric Cry1Ab (10 nM) in solution. Unbound Cry1Ab toxin was estimated by transferring the reaction mixtures to APN-coated ELISA plates by using an anti-Cry1Ab antibody. Insert shows the monomeric Cry1Ab interaction with BBMV.

latter interaction promotes toxin migration and pore formation in DRM.

Several data provided in this study suggest that APN could be involved in toxin insertion into cell membranes by concentrating Cry1Ab oligomeric structure in DRM microdomains:

(1) After BBMV exposure to Cry1Ab protoxin, the 250 kDa oligomeric structure of the toxin was detected in insoluble DRM (Fig. 1B).
(2) Cleavage of APN by PI-PLC substantially decreased the levels of Cry1Ab oligomer in insoluble DRM (Fig. 1C).
(3) Immunoprecipitation of APN after exposure of BBMV to Cry1Ab protoxin showed that Cry1Ab oligomeric structure co-precipitates with APN after longer incubation times (Fig. 2E) suggesting that the oligomeric Cry1Ab is directly associated with APN.
(4) Immunoprecipitation of toxin-binding proteins (APN and BT-R_1) by pure monomeric or oligomeric structures of Cry1Ab toxin showed that APN was preferentially observed after immunoprecipitation with the pure oligomeric toxin structure (Fig. 3). In contrast, Bt-R_1 was preferentially detected when the experiment was done with the monomeric Cry1Ab structure. The binding preference of the oligomeric Cry1Ab to APN receptor is explained by its lower apparent dissociation constant, i.e. higher affinity, in comparison to that shown by the monomer to APN (Fig. 4).

Based on these studies we propose that both receptors are involved in insect toxicity by interacting sequentially with different toxin structures. An updated model of Cry1A toxicity is shown in Fig. 5. After Bt crystal ingestion, the protoxin is solubilized and processed by midgut proteases. In this work, we found that membrane-associated proteases are able to fully activate the protoxin. The C-terminal half and 29 residues of the N-terminus are cleaved at this stage [46], and the activated toxin then binds midgut cell membrane receptors. Based on the different binding affinities of monomeric Cry1A to Bt-R_1 and APN (1 vs. 100 nM, respectively) [7,13], and on the data reported in this study (Fig. 2B), binding to Bt-R_1 is probably the first event in the interaction with the microvilli membrane. This initial binding promotes a conformational change in the toxin facilitating proteolytic cleavage of helix α-1, by a membrane-bound protease [14]. This cleavage results in the formation of a tetrameric pre-pore structure that is insertion competent [14]. The oligomeric toxin then binds APN, which drives the pre-pore complex to DRM lipid rafts where it inserts into the membrane.

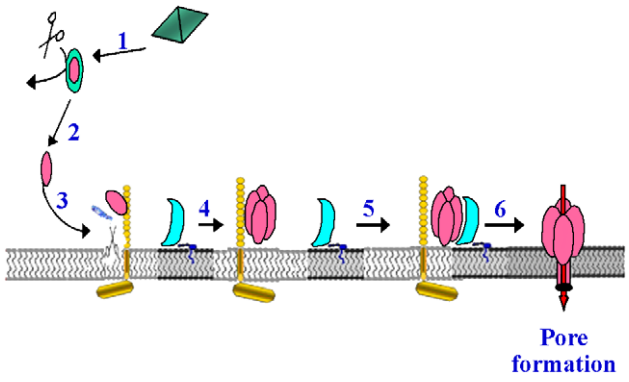

Fig. 5. Model of the mode of action of Cry toxins. (1) Crystal solubilization; (2) protoxin proteolytic activation; (3) monomer binding to Bt-R_1 and cleavage of helix α-1; (4) pre-pore oligomeric structure formation; (5) oligomer binding to APN and mobilization to DRM; (6) pore formation in DRM.

Until now the insect populations selected for their resistance to Cry1A toxins show mutations in the cadherin genes [23,47]. These data indicate that cadherins are important receptors for these Cry1A toxins. However, the fact that in vivo disruption of APN in *S. litura* also resulted in insect resistance to Cry1C toxin [25] supports the idea that APN has an important role in toxin activity. In addition, a resistant line of *Spodoptera exigua* to Cry1Ca toxin did not express the APN gene suggesting that APN could also be involved in toxicity, although the linkage between the resistant phenotype and the lack of APN remains to be determined (de Maagd, R. personal communication). In addition, the expression of only the cadherin-like receptor in mammalian and *Drosophila* cell lines results in low sensitivity at very high toxin levels ([19–22]; Gill, S. unpublished), and only a small proportion of the Bt-R_1 expressing cells are sensitive to Cry1A toxin at these toxin concentrations [21], suggesting that other factor may be missing in these cells or that function of the cadherin receptor is altered due to differences in membrane environment. Moreover, Banks et al. [48] reported that the heterologous production of *H. virescens* APN in S2 *Drosophila* cells did not result in Cry1Ac toxicity, when monomeric Cry1Ac structure was used in the bioassay. It would be interesting to determine the sensitivity of S2 cells producing APN to the oligomeric form of Cry1A toxins.

The involvement of several receptor molecules and the mechanism for sequential interaction could be a common mechanism used by other toxins and viruses. For Cry toxins, which are presently used in transgenic crops, identification of these mechanisms is critical for management of potential insect resistance in the field. Finally, binding of Cry1A toxins to Bt-R_1 and APN receptors are key steps in the mode of action of these toxins. However, the participation of other uncharacterized molecules during the process of membrane insertion and pore formation cannot be excluded.

Acknowledgments

We thank Claudia Morera and Maria Luisa Tabche for technical assistance. This research was supported in part by

DGAPA/UNAM IN216300, CONACyT 36505-N and USDA 2002-35302-12539.

References

[1] E. Schnepf, N. Crickmore, J. Van Rie, D. Lereclus, J. Baum, J. Feitelson, D.R. Zeigler, D.H. Dean, *Bacillus thuringiensis* and its pesticidal crystal proteins, Microbiol. Mol. Biol. Rev. 62 (1998) 775–806.

[2] J. Li, J. Carroll, D.J. Ellar, Crystal structure of insecticidal δ-endotoxin from *Bacillus thuringiensis* at 2.5 Å resolution, Nature 353 (1991) 815–821.

[3] P. Grochulski, L. Masson, S. Borisova, M. Pusztai-Carey, J.L. Schwartz, R. Brousseau, M. Cygler, *Bacillus thuringiensis* Cry1A(a) insecticidal toxin: crystal structure and channel formation, J. Mol. Biol. 254 (1995) 447–464.

[4] R.J. Morse, T. Yamamoto, R.M. Stroud, Structure of Cry2Aa suggests an unexpected receptor binding epitope, Structure 9 (2001) 409–417.

[5] P. Knight, N. Crickmore, D.J. Ellar, The receptor for *Bacillus thuringiensis* CryIA(c) delta-endotoxin in the brush border membrane of the lepidopteran *Manduca sexta* is aminopeptidase, Mol. Microbiol. 11 (1994) 429–436.

[6] S.S. Gill, E.A. Cowles, V. Francis, Identification, isolation, and cloning of a *Bacillus thuringiensis* CryIAc toxin-binding protein from the midgut of the lepidopteran insect *Heliothis virescens*, J. Biol. Chem. 270 (1995) 27277–27282.

[7] S. Sangadala, F.W. Walters, L.H. English, M.J. Adang, A mixture of *Manduca sexta* aminopeptidase and phosphatase enhances *Bacillus thuringiensis* insecticidal CryIA(c) toxin binding and $^{86}Rb^{+}$-K^{+} efflux in vitro, J. Biol. Chem. 269 (1994) 10088–10092.

[8] M.K. Lee, T.H. You, B.A. Young, J.A. Cotrill, A.P. Valaitis, D.H. Dean, Aminopeptidase N purified from gypsy moth brush border membrane vesicles is a specific receptor for *Bacillus thuringiensis* CryIAc toxin, Appl. Environ. Microbiol. 62 (1996) 2845–2849.

[9] R.K. Vadlamudi, E. Weber, I. Ji, T.H. Ji, L.A. Bulla Jr., Cloning and expression of a receptor for an insecticidal toxin of *Bacillus thuringiensis*, J. Biol. Chem. 270 (1995) 5490–5494.

[10] Y. Nagamatsu, T. Koike, K. Sasaki, A. Yoshimoto, Y. Furukawa, The cadherin-like protein is essential to specificity determination and cytotoxic action of the *Bacillus thuringiensis* insecticidal, FEBS Lett. 460 (1999) 385–390.

[11] A. Bravo, S. Jansens, M. Peferoen, Immunocytochemical localization of *Bacillus thuringiensis* insecticidal crystal proteins in intoxicated insects, J. Invertebr. Pathol. 60 (1992) 237–246.

[12] C. Hofmann, H. Vanderbruggen, H. Höfte, J. Van Rie, S. Jansens, H. Van Mellaert, Specificity of *Bacillus thuringiensis* δ-endotoxin is correlated with the presence of high-affinity binding sites in the brush border membrane of target insect midguts, Proc. Natl. Acad. Sci. U. S. A. 85 (1988) 7844–7848.

[13] R.K. Vadlamudi, T.H. Ji, L.A. Bulla Jr., A specific binding protein from *Manduca sexta* for the insecticidal toxin of *Bacillus thuringiensis* subsp. *berliner*, J. Biol. Chem. 268 (1993) 12334–12340.

[14] I. Gómez, J. Sánchez, R. Miranda, A. Bravo, M. Soberón, Cadherin-like receptor binding facilitates proteolytic cleavage of helix α-1 in domain I and oligomer pre-pore formation of *Bacillus thuringiensis* Cry1Ab toxin, FEBS Lett. 513 (2002) 242–246.

[15] C. Rausell, C. Muñoz-Garay, I. Gómez, R. Miranda-CassoLuengo, E. Rudiño-Piñera, M. Soberón, A. Bravo, Tryptophan spectroscopy studies and black lipid bilayer analysis indicate that the oligomeric structure of Cry1Ab toxin from *Bacillus thuringiensis* is the membrane-insertion intermediate, Biochemistry 43 (2004) 166–174.

[16] A. Lorence, A. Darszon, C. Díaz, A. Liévano, R. Quintero, A. Bravo, Delta-endotoxins induce cation channels in *Spodoptera frugiperda* brush border membrane in suspension and in planar lipid bilayers, FEBS Lett. 360 (1995) 217–222.

[17] J. Carroll, D.J. Ellar, Analysis of the large aqueous pores produced by *Bacillus thuringiensis* protein insecticide in *Manduca sexta* midgut-brush-border-membrane vesicles, Eur. J. Biochem. 245 (1997) 797–804.

[18] V. Vie, N. Van Mau, P. Pomarede, C. Dance, J.L. Schwartz, R. Laprade, R. Frutos, C. Rang, L. Masson, F. Heitz, C. Le Grimellec, Lipid-induced pore formation of the *Bacillus thuringiensis* Cry1Aa insecticidal toxin, J. Membr. Biol. 180 (2001) 195–203.

[19] J.A. Dorsch, M. Candas, N.B. Griko, W.S.A. Maaty, E.G. Midbo, R.K. Vadlamudi, L.A. Bulla Jr., Cry1A toxins of *Bacillus thuringiensis* bind specifically to a region adjacent to the membrane-proximal extracelullar domain of Bt-R_1 in *Manduca sexta*: involvement of a cadherin in the entomopathogenicity of *Bacillus thuringiensis*, Insect Biochem. Mol. Biol. 32 (2002) 1025–1036.

[20] Y. Tsuda, F. Nakatani, K. Hashimoto, S. Ikawa, C. Matsura, T. Fukada, K. Sugimoto, M. Himeno, Cytotoxic activity of *Bacillus thuringiensis* Cry proteins on mammalian cells transfected with cadherin-like Cry receptor gene of *Bombyx mori* (silkworm), Biochem. J. 369 (2003) 697–703.

[21] G. Hua, J.L. Jurat-Fuentes, M.J. Adang, Fluorescent-based assays establish *Manduca sexta* Bt-R(1a) cadherin as a receptor for multiple *Bacillus thuringiensis* Cry1A toxins in *Drosophila* S2 cells, Insect Biochem. Mol. Biol. 34 (2004) 193–202.

[22] H. Hara, S. Atsumi, K. Yaoi, S. Higurashi, N. Miura, H. Tabunoki, R. Sato, A cadherin-like protein functions as a receptor for *Bacillus thuringiensis* Cry1Aa and Cry1Ac toxins on midgut epithelial cells of *Bombyx mori* larvae, FEBS Lett. 538 (2003) 29–34.

[23] L.J. Gahan, F. Gould, D.G. Heckel, Identification of a gene associated with Bt resistance in *Heliothis virescens*, Science 293 (2001) 342–350.

[24] R. Miranda, F.Z. Zamudio, A. Bravo, Processing of Cry1Ab δ-endotoxin from *Bacillus thuringiensis* by midgut proteases: role in toxin activation and inactivation, Insect Biochem. Mol. Biol. 31 (2001) 1155–1163.

[25] R. Rajagopal, S. Sivakumar, N. Agrawal, P. Malhotra, R.K. Bhatnagar, Silencing of midgut aminopeptidase N of *Spodoptera litura* by double-stranded RNA establishes its role as *Bacillus thuringiensis* toxin receptor, J. Biol. Chem. 277 (2002) 46849–46851.

[26] M. Gill, D.J. Ellar, Transgenic *Drosophila* reveals a functional in vivo receptor for the *Bacillus thuringiensis* toxin Cry1Ac1, Insect Mol. Biol. 11 (2002) 619–625.

[27] J.L. Schwartz, Y.J. Lu, P. Sohnlein, R. Brousseau, R. Laprade, L. Masson, M.J. Adang, Ion channels formed in planar lipid bilayers by *Bacillus thuringiensis* toxins in the presence of *Manduca sexta* midgut receptors, FEBS Lett. 412 (1997) 270–276.

[28] A. Lorence, A. Darszon, A. Bravo, The pore formation activity of *Bacillus thuringiensis* Cry1Ac toxin on *Trichoplusia ni* membranes depends on the presence of aminopeptidase N, FEBS Lett. 414 (1997) 303–307.

[29] R.J. Schroeder, S.N. Ahmed, Y. Zhu, E. London, D.A. Brown, Cholesterol and sphingolipid enhance the Triton X-100 insolubility of glycosylphosphatidylinositol-anchored proteins by promoting the formation of detergent-insoluble ordered membrane domains, J. Biol. Chem. 273 (1998) 1150–1157.

[30] C.M. Rosenberger, J.H. Brumell, B.B. Finlay, Microbial pathogenesis: lipid rafts as pathogen portals, Curr. Biol. 10 (2000) 823–825.

[31] V. Cabiaux, Ch. Wolff, J.M. Ruysschaert, Interaction with a lipid membrane: a key step in bacterial toxins virulence, Int. J. Biol. Macromol. 21 (1997) 285–298.

[32] M. Zhuang, D.I. Oltean, I. Gómez, A.K. Pullikuth, M. Soberón, A. Bravo, S.S. Gill, *Heliothis virescens* and *Manduca sexta* lipid rafts are involved in Cry1A toxin binding to the midgut epithelium and subsequent pore formation, J. Biol. Chem. 277 (2002) 13863–13872.

[33] O. Arantes, D. Lereclus, Construction of cloning vectors for *Bacillus thuringiensis*, Gene 108 (1991) 115–119.

[34] J.L. Jenkins, M.K. Lee, A.P. Valaitis, A. Curtiss, D.H. Dean, Bivalent sequential binding model of a *Bacillus thuringiensis* toxin

to gypsy moth aminopeptidase N receptor, J. Biol. Chem. 275 (2000) 14423–14431.
[35] F. Hardy, L. Djavadi-Ohaniance, M.E. Goldberg, Measurement of antibody/antigen association rate constants in solution by a method based on the enzyme-linked immunosorbent assay, J. Immunol. Methods 200 (1997) 155–159.
[36] L. Dong, S. Chen, U. Bartsch, M. Schachner, Generation of affinity matured scFv antibodies against mouse neural cell adhesion molecule L1 by phage display, Biochem. Biophys. Res, Commun. 301 (2003) 60–70.
[37] D.J. Lightwood, D. Ellar, P. Jarrett, Role of proteolysis in determining potency of *Bacillus thuringiensis* Cry1Ac δ-endotoxin, Appl. Environ. Microbiol. 66 (2000) 5174–5181.
[38] M. Sharon, N. Kessler, R. Levy, S. Zolla-Pazner, M. Görlach, J. Anglister, Alternative conformations of HIV-1 V3 loops mimic β haipins in chemokines, suggesting a mechanism for coreceptor selectivity, Structure 11 (2003) 225–236.
[39] B. Bartosch, A. Vitelli, C. Granier, C. Goujon, J. Dubuisson, S. Pascale, E. Scarselli, R. Cortese, A. Nicosia, F.L. Cosset, Cell entry of hepatitis C virus requires a set of co-receptors that include the CD81 tetraspanin and the SR-B1 scavenger receptor, J. Biol. Chem. 278 (2003) 41624–41630.
[40] G.R. Nemerow, Cell receptors involved in adenovirus entry, Virology 274 (2000) 1–4.
[41] Y. Shen, M. Naujokas, M. Park, M.K. Ireton, InlB-dependent internalization of *Listeria* is mediated by the Met receptor tyrosine kinase, Cell 103 (2003) 501–510.
[42] H.M. Scobie, G.J.A. Rainey, K.A. Bradley, J.A.T. Young, Human capillary morphogenesis protein 2 functions as an anthrax toxin receptor, Proc. Natl. Acad. Sci. U. S. A. 100 (2003) 5170–5174.
[43] L. Abrami, M. Fivaz, F.G. van der Goot, Adventures of a pore-forming toxin at the target cell surface, Trends Microbiol. 8 (2000) 168–172.
[44] L. Abrami, M. Fivaz, P.E. Glauser, N. Sugimoto, C. Zurzolo, F.G. van der Goot, Sensitivity of polarized epithelial cells to the pore-forming toxin aerolysin, Infect. Immun. 71 (2003) 739–746.
[45] H. Hasuwa, Y. Shishido, A. Yamazaki, T. Kobayashi, X. Yu, E. Mekada, CD9 amino acids critical for up regulation of diphtheria toxin binding, Biochem. Biophys. Res. Commun. 289 (2001) 782–790.
[46] A. Bravo, J. Sánchez, T. Kouskoura, N. Crickmore, N-terminal activation is an essential early step in the mechanism of action of the *B. thuringiensis* Cry1Ac insecticidal toxin, J. Biol. Chem. 277 (2002) 23985–23987.
[47] S. Morin, R.W. Biggs, M.S. Sisterson, L. Shriver, C. Ellers-Kirk, D. Higginson, D. Holley, L.J. Gahan, D.G. Heckel, Y. Carriere, T.J. Dennehy, J.K. Brown, B.E. Tabashnik, Three cadherin alleles associated with resistance to *Bacillus thuringiensis* in pink bollworm, Proc. Natl. Acad. Sci. 100 (2003) 5004–5009.
[48] D.J. Banks, G. Hua, M.J. Adang, Cloning of a *Heliothis virescens* 110 kDa aminopeptidase N and expression in *Drosophila* S2 cells, Insect Biochem. Mol. Biol. 33 (2003) 499–508.